International Journal of Pharmaceutics 410 (2011) 99–106

Contents lists available at ScienceDirect

International Journal of Pharmaceutics

journal homepage: www.elsevier.com/locate/ijpharm

Variability in commercial carbamazepine samples – Impact on drug release

Felicia Flicker, Veronika Anna Eberle, Gabriele Betz*

Industrial Pharmacy Lab, University of Basel, Mülhauserstrasse 51, Basel 4056, Switzerland

ARTICLE INFO

Article history:
Received 16 December 2010
Received in revised form 1 March 2011
Accepted 13 March 2011
Available online 22 March 2011

Keywords:
Carbamazepine
Dihydrate
Preformulation
Morphology
Polymorphism
Tablet filler

ABSTRACT

The aim of this study was to characterize the variability of commercial carbamazepine (CBZ) samples and to investigate the influence of two commonly used tablet fillers, i.e., mannitol and microcrystalline cellulose (MCC) on the CBZ sample variability. Polymorphism and morphology of CBZ samples were analyzed by differential scanning calorimetry, X-ray powder diffraction, sieve analysis, and scanning electron microscopy. Drug release from CBZ samples and binary mixtures (30–90% drug load) was characterized by a unidirectional dissolution method measuring disk intrinsic dissolution rate (DIDR) and drug release, respectively. All CBZ samples were of p-monoclinic form but differed in their polymorphic purity, particle size, morphology and intrinsic dissolution rate. Two characteristic inflection points, determined in the DIDR profiles, characterized the specific transformation behavior of each CBZ sample. The variability in CBZ samples was also exhibited in the drug release profiles from their binary mixtures. Mannitol increased initial drug release of CBZ samples up to 10-fold in mixtures of 30% drug load. The presence of MCC resulted in reduced variability in drug release. The unidirectional dissolution method is presented as a straightforward monitoring tool to characterize variability of CBZ raw materials and effect of tablet fillers.

1. Introduction

Carbamazepine (CBZ) is a well-established drug to treat epilepsy and trigeminal neuralgia and there are already several generics on the market. Nevertheless, CBZ products present a history of irregular drug performance and clinical failures. Several reports show high dissolution variability in CBZ tablets on the market worldwide and even among CBZ tablets of the same brand (Meyer et al., 1992, 1998; Davidson, 1995; Al-Zein et al., 1999; Lake et al., 1999; Mittapalli et al., 2008).

CBZ is poorly soluble in water with a narrow therapeutic index, classified as class 2 drug according to the Biopharmaceutics Classification System (Lindenberg et al., 2004). Furthermore, CBZ exhibits at least four polymorphic forms referring to p-monoclinic (form III), triclinic (form I), c-monoclinic (form IV), and trigonal (form II) crystal lattice. At room temperature CBZ form III is the thermodynamically most stable form and also the form commercially available. CBZ further exists as several solvates, e.g., CBZ monoacetonate (Fleischman et al., 2003). Both, CBZ polymorphs and solvates show differences in crystal form and consequently also difference in melting point, solubility, compactability, and chemical reactivity.

Information about the processes used in raw drug production is generally limited. Polymorphic form may be the same among various commercial sources, however, different solvents and additives can be used for the crystallization of drug raw materials. These dissimilar processes lead to different crystal habits and possible solvent inclusions, which result in changed solubility and dissolution behavior of CBZ crystals (Mahalaxmi et al., 2009; Blagden et al., 2007; Bolourtchian et al., 2001). Furthermore, physical processes, such as milling or grinding, can cause crystal defects, mechanical activation, and small amount of amorphous, which then also lead to faster and inhomogenous dissolution behavior of CBZ samples (Tian et al., 2006b; Murphy et al., 2002; Mosharraf et al., 1999; Lefebvre et al., 1986).

In aqueous media, anhydrous CBZ transforms into its dihydrate. This transformation critically influences dissolution and bioavailability of CBZ formulations and it has been in the focus of many investigations over the last 20 years. The mechanism of transformation is a solution-mediated process where dihydrate is formed by whisker growth, clearly visible by optical microscopy (Laine et al., 1984). Raman spectroscopy and fluorescence studies are presented as non invasive methods to study the transformation behavior of CBZ (Tian et al., 2006a,b; Brittain, 2004). Furthermore, the influence of transformation on the dissolution rate has been investigated. A decrease in dissolution rate is expected as soon as the less soluble CBZ dihydrate is formed. This phenomenon is detected as an inflection point in the disk intrinsic dissolution rate (DIDR) profile of CBZ samples (Kobayashi et al., 2000; Šehić et al., 2010). Kobayashi et al. (2000) reported that the transformation depends on the polymorphic form. CBZ form I transforms faster to dihy-

* Corresponding author. Tel.: +41 61 381 07 20; fax: +41 61 381 04 30.
E-mail address: gabriele.betz@unibas.ch (G. Betz).

0378-5173/$ – see front matter © 2011 Elsevier B.V. All rights reserved.
doi:10.1016/j.ijpharm.2011.03.032

drate than form III in vitro and results in lower bioavailability in vivo. Šehić et al. (2010), however, reported different transformation points within commercial CBZ samples, though same polymorphic form was specified. This difference also shows in tablet formulation using Ludipress® as tablet filler. To date, DIDR profiles focused on the onset of transformation only.

Composition of the dissolution media also influences the transformation of CBZ. Dihydrate formation is strongly inhibited in solutions (1–4%, w/v) of hydroxypropyl methylcellulose (HPMC), hydroxypropylcellulose (HPC), or polyvinylpyrrolidone (PVP) whereas solutions of polyvinyl alcohol (PVA), polyethylene glycol (PEG), and sodium carboxymethylcellulose (CMC) have only weak inhibitory activity (Gift et al., 2008; Tian et al., 2006a; Otsuka et al., 2000). In contrast, surfactants, such as sodium lauryl sulphate and sodium taurocholate promote the dihydrate formation during the dissolution test (Rodrìguez-Hornedo and Murphy, 2004). Nevertheless, the knowledge about the effect of commonly used tablet fillers is still limited (Salameh and Taylor, 2006).

In this study, a unidirectional dissolution method was developed building on the DIDR method of Šehić et al. (2010) to characterize CBZ samples by DIDR profiles of the transformation range and to investigate their initial drug release of binary mixtures with commonly used tablet fillers. For this purpose, two different types of direct compacted filler were selected, mannitol as water soluble and microcrystalline cellulose (MCC) as water insoluble tablet filler.

2. Materials and methods

CBZ samples were obtained from four different suppliers; for confidential reasons they were designated as CBZ A, B, C, and D. All samples were of commercial grade, no further specification for the drug substance was made from our side. Samples were stored at room temperature (20–25 °C) and controlled relative humidity (43% RH). *CBZ dihydrate* was prepared according to McMahon et al. (1996). Anhydrous CBZ was stirred in water for 24 h. Crystals were filtered under suction and dried at ambient conditions over night. The obtained CBZ dihydrate was kept at room temperature and 80% RH.

Excipients for the binary mixtures: Mannitol (Parteck® M300, MERCK KGaA, Germany) and microcrystalline cellulose (MCC SANAQ® 102L, Pharmatrans SANAQ AG, Switzerland) were used as the tablet fillers. All other chemicals and reagents purchased from commercial sources were of analytical grade.

2.1. Morphological characterization

For morphological characterization scanning electron microscopy (SEM) (ESEM XL 30 FEG, Philips, The Netherlands) were applied at a voltage of 10 kV and magnifications of 100–2000 times. Before analysis, powder was sprinkled on carbon adhesive, and compacts were fixed to the sample holder by conductive silver. The samples were then sputtered with gold.

Sieve analysis was performed with 100 g samples on standard sieving tower (Retsch Type Vibro, Schieritz & Hauenstein AG, Switzerland) and 10 min shaking time at 40 Hz.

2.2. Polymorphic characterization

Polymorphic form of CBZ samples was characterized by X-ray powder diffractometry (XRPD) using a diffractometer (D5000, Siemens, Germany). The powder was filled into special holders and the surface was pressed flat. Operating conditions were Ni filtered Cu Kα radiation (λ = 1.5406 Å), 40 kV, and 30 mA. Step was 0.02° 2θ, step time 1.0 s, angular scanning speed 1° 2θ/min, and angular range between 5° and 40° 2θ scale.

Thermal behavior of all samples was analyzed by differential scanning calorimetry (DSC), using heat flux DSC (4000, PerkinElmer, USA). DSC was calibrated with indium prior to the measurement. A sample of 3–6 mg was accurately weighted into an aluminum pan with holes and scanned between 40 °C and 220 °C at 10 °C/min under dry nitrogen gas purge (20 ml/min).

True density of all samples was assessed by a gas displacement pycnometer (AccuPyc 1330, Micromeritics, USA). Powder was purged with helium by five repetitive purging cycles and the density was reported as average value. The test was performed in triplicate.

2.3. Water activity measurement

Water activity (a_W) is the partial vapor pressure (p) of a sample relative to the vapor pressure of pure water (p_0). It is equal to the equilibrium relative humidity (ERH) of air over the sample, e.g., powder or tablets (Wrolstad et al., 2005); see Eq. (1). All parameters are temperature dependent.

$$a_W = \frac{p}{p_0} = \text{ERH} \quad (1)$$

Water activity of all samples was monitored with the digital water activity analyzer (Hygropalm, Rotronic AG, Switzerland) at 23.5 ± 1.5 °C.

2.4. Intrinsic dissolution of CBZ samples

CBZ samples were analyzed by disk intrinsic dissolution. Intrinsic dissolution rate (IDR) is the specific dissolution rate of a pure drug from one surface only. IDR is described by Eq. (2),

$$\text{IDR} = \frac{dC}{dt} \times \frac{V}{S} = k \times C_S \quad (2)$$

where dC/dt is the amount of drug dissolving over time, V is the dissolution volume, S the surface area of the compact, k the intrinsic dissolution constant, and C_S the solubility of the drug. Disc intrinsic dissolution curves are linear and the slope is the amount of drug dissolved per cm^2. Under fixed experimental conditions IDR value is characteristic for a given substance. It is used in preformulation studies to classify and predict possible problems in bioavailability of a drug (Zakeri-Milani et al., 2009; Hanson and Gray, 2004).

2.4.1. Sample preparation

Flat-faced compacts of 400 mg and 0.95 cm^2 surface area were produced from CBZ samples and CBZ dihydrate using a material tester (Zwick 1478, Germany). Compact porosity was controlled to 11.3 ± 0.7% and hardness was 20–41 N. For compacts of CBZ A, porosity was 16%, as higher compaction forces resulted in lamination. Compaction force was set between 6 and 10 kN, while compaction, decompaction, and ejection speed were set at 10 mm/min, 50 mm/min, and 10 mm/min, respectively.

Porosity of CBZ compacts was measured by a mercury porosimeter (AutoPore 4 9500, Micrometrics, USA). Pressure in the range of 0.014–0.227 MPa corresponding to the mean pore diameter of 6 nm to 400 μm, was applied. Surface tension (γ) of mercury was 485 dynes/cm and contact angle (θ) was 130.

2.4.2. Unidirectional dissolution method

To obtain disk intrinsic dissolution rate (DIDR) profiles of the CBZ samples unidirectional dissolution was performed by a modified USP Apparatus 1. The compact was placed in a sample holder fitting to the rotating unit of the dissolution apparatus (SotaxAT7*smart*, SOTAX AG, Switzerland) and the compact was embedded in melted paraffin that only one surface was available to the dissolution media. Unidirectional dissolution method was performed at two

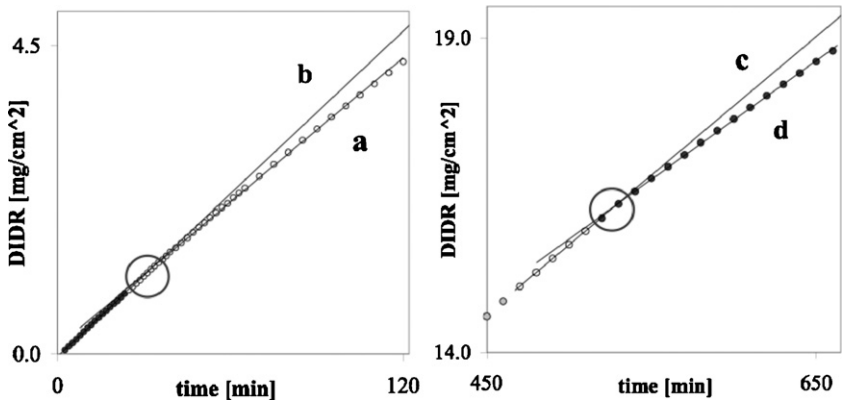

Fig. 1. Inflection point in DIDR profiles of 2-h run (left) and 10–11-h run (right) determined by the intercept of slope a and b, and slope c and d, respectively. In the 10–11-h run only every second data point is shown.

conditions: one for the analysis of first inflection point referring to the start of transformation, and another for the second inflection point referring to the stabilized transformation rate. Release media was 500 ml and 1000 ml water, and run time was 2 h and 10–11 h for these two conditions, respectively. Dissolution media was at 37 ± 0.5 and a rotation speed of 100 rpm was selected as it showed the lowest standard deviation for drug release of each sample. Drug content of the media was measured at predetermined time intervals by UV/VIS spectrophotometer (Lambda 25, PerkinElmer, USA) at 285 nm.

2.4.3. Evaluation of DIDR profiles

IDR was determined by the slope in the DIDR profile prior to the first inflection point, the slope referring to the release of anhydrous CBZ before transforming to the dihydrate.

The inflection point was determined by the intercept of two linear regressions with the best fit ($R^2 \geq 0.999$). The linear regressions *a* and *b* in the DIDR profiles of 2-h run and *c* and *d* in the profiles of 10–11-h run were used to determine the first and second inflection point, respectively (Fig. 1). For the first inflection point, approximation of the best linear regression (*a*) included the initial DIDR profile starting from 2.6 min DIDR measurement. The linear regression *b* was set through all data points of the later stage in the DIDR profile that were not included in the regression line *a*. For the second inflection point, approximation of the best linear regression (*d*) included the late stage in DIDR profile, where release rate stabilized. The linear regression *c* was set through the ten preceding release values not included in regression *d*.

2.5. Binary mixtures

CBZ samples were mixed with mannitol or MCC for 10 min in a mixer (Turbula® type T2C, W. Bachofen, Switzerland) and for a further 2 min after adding 1% magnesium stearate (Sandoz, Switzerland) to the mixture. Drug loads were set at 90%, 70%, 50%, and 30% and mixtures of 20 g were prepared. Binary mixtures were compacted by the same procedure as the compaction of CBZ samples at the condition of 50 mm/min, 100 mm/min, and 50 mm/min

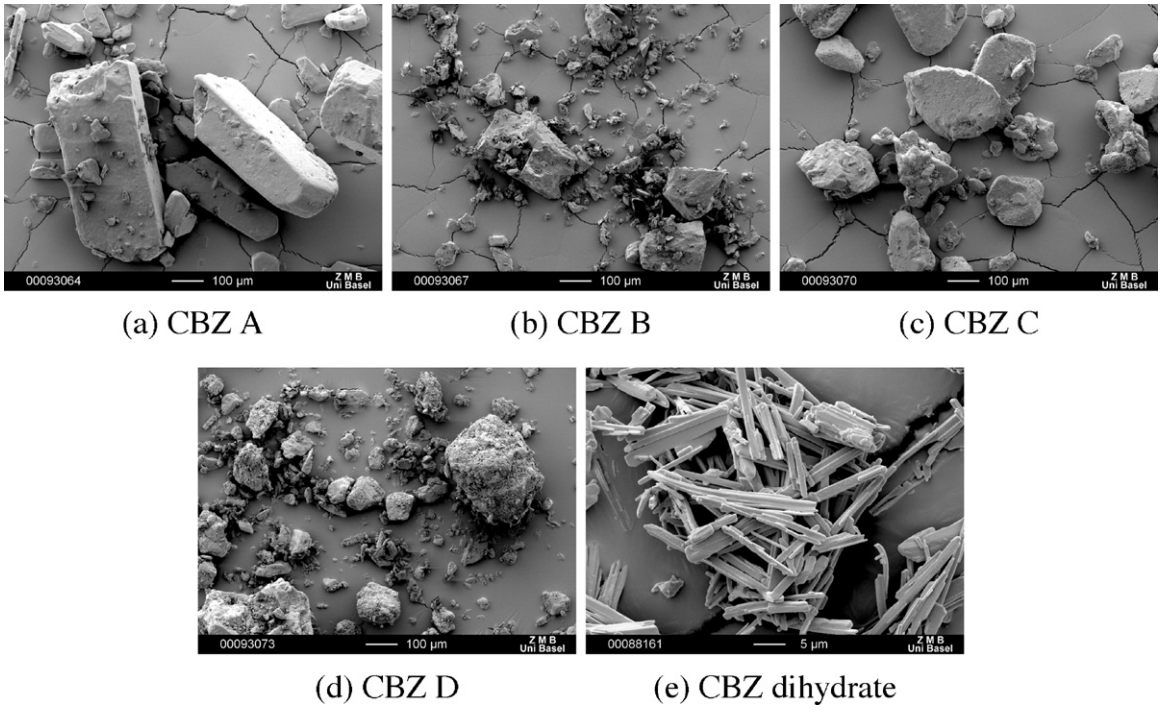

Fig. 2. SEM pictures of CBZ samples and CBZ dihydrate.

Table 1
Sieve fractions of CBZ in [%] total sample weight ($n = 3$).

μm	CBZ A	CBZ B	CBZ C	CBZ D
≥710	0.5	0.1	3.1	2.8
500–710	3.5	0.1	11.8	26.5
355–500	10.7	1.2	11.3	17.2
250–355	23.8	16.2	15.4	17.5
180–250	20.9	23.0	10.4	10.3
125–180	21.3	24.9	20.0	7.9
90–125	12.1	13.2	15.3	6.9
≤90	7.3	21.4	12.8	11.0
Average	233 ± 5	166 ± 4	241 ± 21	333 ± 32
Median	209 ± 9	155 ± 4	192 ± 8	331 ± 20

for compaction, decompaction, and ejection speed, respectively. Porosity was kept at approximately 12% based on tablet volume. To compare drug release of the binary mixtures and CBZ samples, initial drug release of binary mixtures was tested by the dissolution method of 2 h (Section 2.4.2). Drug release profiles of binary mixtures were compared by the amount of drug dissolved after 120 min dissolution test.

For all statistical comparison, one-way ANOVA followed by Student's *t*-test was applied.

3. Results and discussion

3.1. Morphological characterization

With SEM a difference in morphology and surface texture was clearly visible among the CBZ samples; see Fig. 2. CBZ A showed very crystalline particles of prismatic shape, whereas CBZ B and D showed particles with rough and uneven edges and a lot of fine particles. Samples of CBZ C were more round and with smoother surface. Prismatic shape was reported characteristic for CBZ form III (Krahn and Mielck, 1987). CBZ dihydrate powders were of fine needle-like structure in loose aggregates as expected (Šehić et al., 2010).

CBZ samples also differed in particle size distribution, in average and in median particle size, see Table 1. CBZ A and D showed monomodal particle size distribution with a very broad peak found in CBZ D. For CBZ B and C, particle size distribution was bi-modal showing two maxima at 0–90 μm and 125–180 μm, and at 125–180 μm and 250–355 μm, respectively. All CBZ samples except for CBZ A contained fines (particle size ≤ 90 μm) of at least 11% with the ranking of CBZ B > C > D > A.

3.2. Polymorphic characterization

XRPD results are shown in Fig. 3. The diffractograms of all CBZ samples showed the characteristic peaks reported for CBZ p-monoclinic (Getsoian et al., 2008; Grzesiak et al., 2003). Peaks at

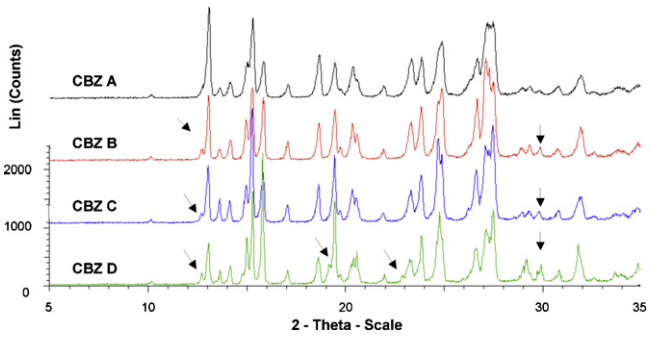

Fig. 3. X-ray powder diffraction of CBZ samples; 5–40° 2θ at 1° 2θ/min.

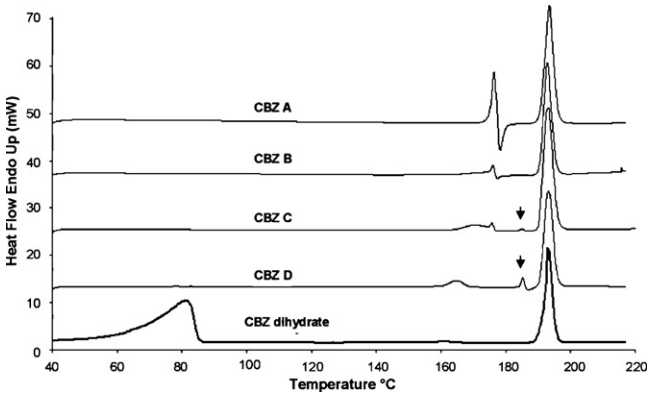

Fig. 4. DSC profiles of CBZ samples and CBZ dihydrate; 40–220 °C at 10 °C/min.

angles smaller than 10, indicating presence of CBZ trinclinic or the trigonal form, were not detected. However, there were some indications as to the presence of form IV. There are peaks at 12.68° and 29.91° 2θ with increasing intensity for CBZ B, C, and D. Diffractograms of CBZ D further showed an extra peak at 19.15°, and at 22.91° 2θ (see arrows). The presence of CBZ form IV in commercial CBZ samples was suspected previously (Kipouros et al., 2005). At lower angles of 5–20° 2θ, XRPD results showed difference in peak intensities, which could be due to different degree in crystallinity, smaller particle size or due to preferred orientation of the particles in the sample holder. XRPD data did not show any change in the diffraction pattern in CBZ samples after compaction (data not shown). CBZ dihydrate was also confirmed by XRPD. Characteristic peaks for CBZ dihydrate were at 2θ = 8.9°, 18.9°, and 19.4°, and they are in agreement with the literature (Kobayashi et al., 2000).

DSC results are presented in Fig. 4. Most CBZ samples showed the characteristic thermal events of CBZ form III as reported previously (Grzesiak et al., 2003). The onset of each thermal event (T_{onset}) and the enthalpy (ΔH) were used to compare the endothermic and exothermic peaks among the CBZ samples. Melting of form III was visible around 176 °C, followed by crystallization to form I around 182 °C and melting of form I around 191 °C. However, DSC profiles of CBZ samples differed visibly. Thermograms of CBZ A and B showed the characteristic peaks for form III clearly. However, there was a difference in melting enthalpy around 176 °C (form III), whereas melting enthalpy around 191 °C (form I) was the same. This indicates presence of form I in CBZ B. Nonetheless, only small amounts can be assumed, as no specific peaks for form I were detected by XRPD. Further difference among CBZ samples was seen for CBZ D, where the endothermic peak around 176 °C was missing and an endotherm showed at lower temperature of around 164 °C instead. For both, CBZ C and D samples a further endothermic peak was visible at 185 °C (arrows) indicating presence of CBZ form IV (Grzesiak et al., 2003). This finding is consistent with the XRPD results, where small amounts of form IV were suspected in both CBZ C and D. However, for CBZ B, no indications of form IV were detected by DSC. It has to be noted here, that the detection limit for CBZ polymorphic form is reported to be the best with 1% and 5–10% for Hyper-DSC and XRPD, respectively (McGregor et al., 2004; Lefebvre et al., 1986). Furthermore, thermograms for CBZ B and C showed a shoulder to the endothermic peak around 176 °C starting around 164 °C. This shoulder has been identified to be due to a direct solid–solid conversion of form III to form I (Zeitler et al., 2007). Deviations in thermal behavior can further be due to solvent inclusion in crystal pores, contamination by other polymorphic form, and amorphous traces. CBZ dihydrate had two endothermic events in DSC measurements. Dehydration was visible as a wide endothermic peak in temperature range of 50–85 °C. Second endothermic peak was at 192 °C showing melting of CBZ from I.

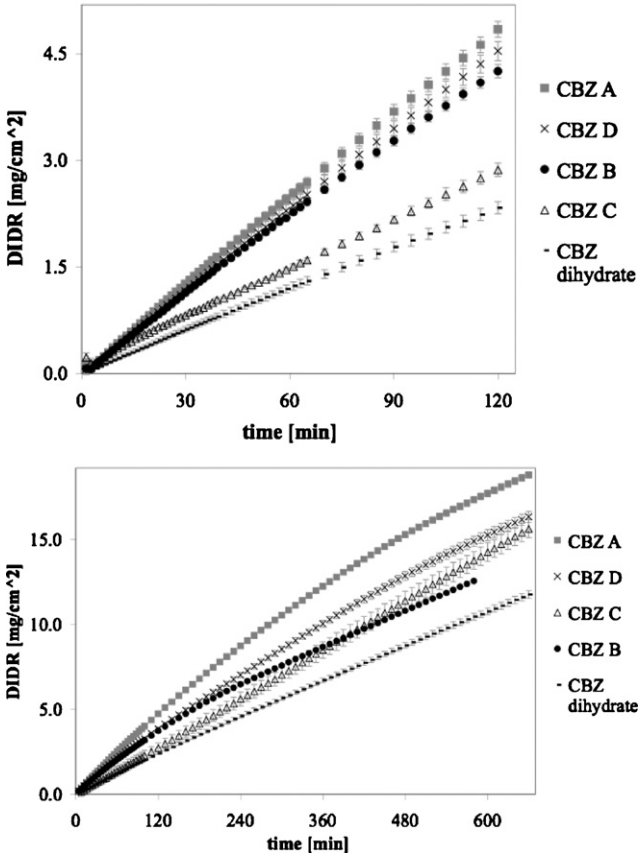

Fig. 5. DIDR profiles of pure carbamazepine from suppliers A, B, C, and D; 2 h (top) and 10–11 h (bottom) dissolution time. Average values ($n \geq 3$) are presented.

Table 2
Intrinsic dissolution rate of CBZ samples and CBZ dihydrate (CBZ dihyr) in the initial DIDR values prior to the first inflection point.

Sample $n \geq 3$	IDR [μg/cm²/min]
CBZ A	43.9 ± 3.1
CBZ B	38.6 ± 0.8
CBZ C	24.0 ± 0.4
CBZ D	39.9 ± 0.7
CBZ dihyr	19.5 ± 0.7

True density of all CBZ samples was 1.338 ± 0.001 g/cm^3 indicating CBZ polymorphic form III (Krahn and Mielck, 1989; Grzesiak et al., 2003).

3.3. Water activity

For all CBZ anhydrous samples water activity was between 0.241 and 0.423. At a specific water activity hydration of drug can occur (Qiu et al., 2009). Also the phase conversion of anhydrous CBZ to CBZ dihydrate depends on the water activity of the system. In the water activity range of 0.601–0.641 at 20 °C CBZ form III and CBZ dihydrate are reported to coexist in equilibrium (Qu et al., 2006; Li et al., 2008). Our samples were therefore below the critical range for transformation.

3.4. DIDR profiles of CBZ samples

DIDR profiles of the four CBZ samples and the CBZ dihydrate are shown in Fig. 5 and Table 2 presents the IDR values. Initial phase in DIDR profiles showed a significant difference in IDR for each CBZ samples ($p < 0.05$). IDR was in the rank of CBZ A > D > B > C and the IDR values were in the same range (29, 35.5, and 37.6 μg/cm²/min) as reported previously (Yu et al., 2004; Zakeri-Milani et al., 2009; Murphy et al., 2002). IDR value of CBZ dihydrate was 1.2–2.2 times lower than for anhydrous CBZ samples. The comparatively low dissolution rate of CBZ C might be explained by presence of small amounts of the less soluble CBZ form IV and compact hardness. CBZ C compacts showed breaking strength about 2 times higher than of the other compacts.

Table 3
First and second inflection point in DIDR profiles of CBZ samples.

Sample $n \geq 3$	First inflection point (min)	Second inflection point (min)
CBZ A	33 ± 6	570 ± 25
CBZ B	28 ± 10	443 ± 93
CBZ C	16 ± 3	350 ± 11
CBZ D	41 ± 7	635 ± 19

It is interesting to note, that the amount of drug dissolved after 120 min inversely correlated with the amount of fines in the CBZ samples. Generally, samples with higher amount of fines show faster dissolution rate, in case of CBZ, however, the opposite was the case. This leads to the conclusion, that CBZ fines transformed faster to the slower dissolving CBZ dihydrate and therefore decreased the actual amount of drug dissolved after 120 min.

3.4.1. Inflection point

DIDR profiles showed not only one point of transformation at the early stage of dissolution, but transformation continued over a time range stabilizing at a later stage within 10 h. The results for the first and second inflection points are shown in Table 3. First inflection points were in the same range as reported previously (Šehić et al., 2010; Kobayashi et al., 2000). CBZ samples differed significantly in their first and second inflection point ($p < 0.05$). Both inflection points could be ranked as C ≤ B < A < D. The ranking was significant only for the second inflection point ($p < 0.05$), except for CBZ B over C ($p = 0.059$). CBZ B showed the highest standard deviation for both inflection points, which might be due to the high amount of fines.

The two inflection points could describe the transformation process from CBZ anhydrous to dihydrate in dissolution. The first inflection point reflected the onset of the gradual change in dissolution rate induced by the forming and dissolution of CBZ dihydrate. The second inflection point reflected onset of the constant dissolution rate, where the transformation process and dissolution were in equilibrium. Transformation as a process over time has been studied on CBZ compact surface during intrinsic dissolution by in situ Raman spectroscopy (Lehto et al., 2008). Based on the knowledge of previous studies gained by Raman spectroscopy, fluorescence studies or XRPD (Tian et al., 2006a; Brittain, 2004; Suryanarayanan, 1989), the transformation range could be derived from the DIDR profiles and thereby characterize the CBZ samples. To confirm the formation of CBZ dihydrate compact surfaces were analyzed by SEM at several time points in DIDR test as described in the following section.

3.4.2. Surface change of CBZ compacts during DIDR test

To avoid recrystallization due to sample preparation, the CBZ compacts were removed from the samples holder inclusive the paraffin layer and gently placed upside down on a kitchen paper for a few seconds. Samples were then kept under controlled RH of 43% for a maximum of 24 h prior the the analysis. SEM pictures of the compact surfaces after 30, 60, 120, and 480 min DIDR test confirmed CBZ dihydrate formation, see Fig. 6. The needle-shaped dihydrate crystals on compact surface were visible at a later stage in DIDR test than their onset of dissolution in the DIDR profiles. Dihydrate was first visible on the CBZ B and D compacts after 60 min and on CBZ A and C compacts after 120 min. CBZ dihydrate crystals

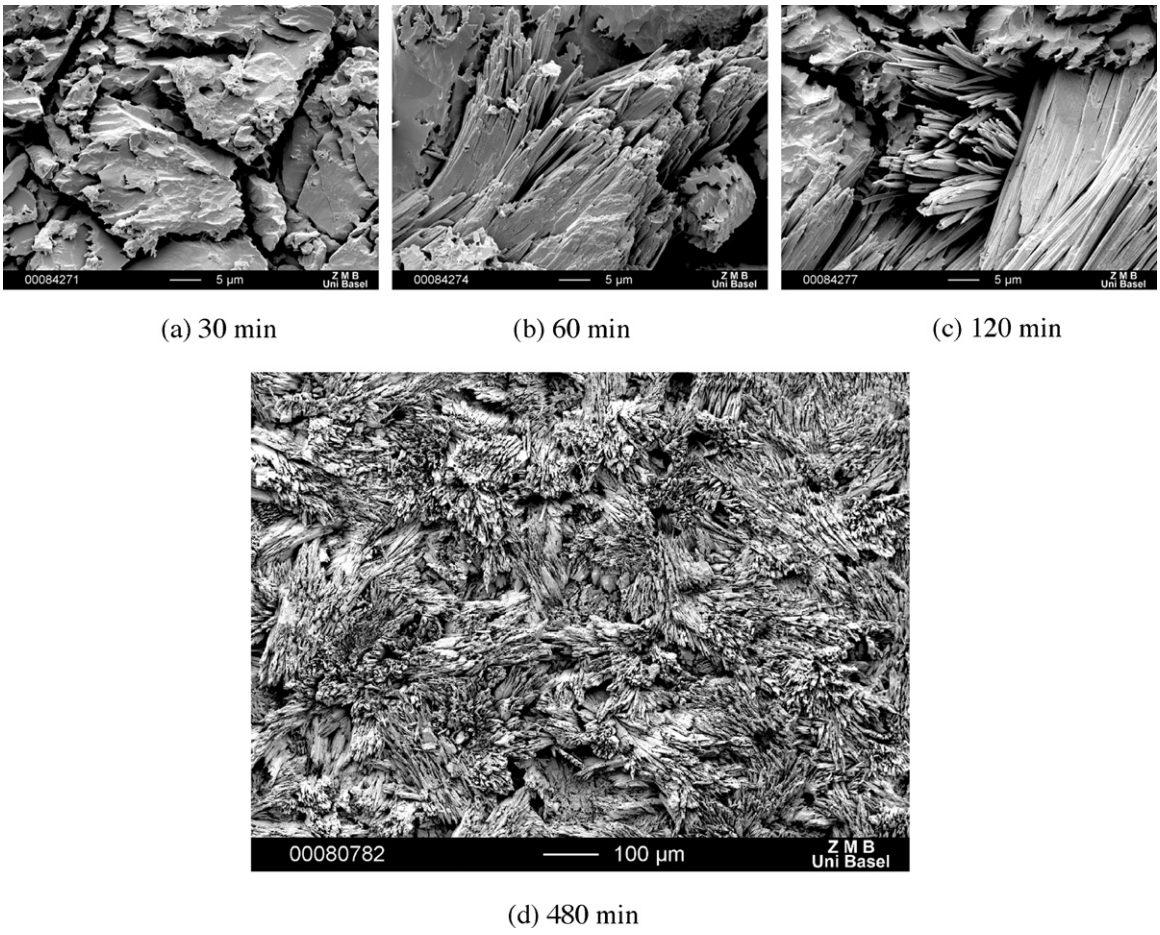

Fig. 6. SEM pictures of compact surface from CBZ B during DIDR test.

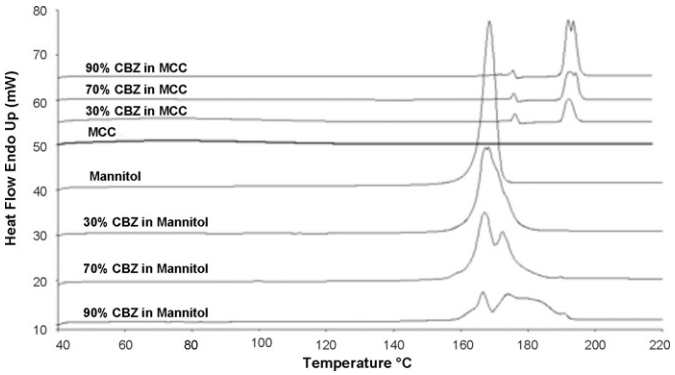

Fig. 7. DSC profiles of binary mixtures of CBZ B in MCC and mannitol; 40–220 °C at 10 °C/min.

grow at disrupted crystal structure of CBZ anhydrate induced, e.g., by grinding (Murphy et al., 2002). CBZ B and D showed the most irregular particle shapes in SEM, they were therefore expected to have the most crystal defects and transform the fastest. For CBZ D, however, the first inflection point showed later compared to the other samples. A reason could be that CBZ D showed less fines compared to CBZ B. The amount of fines may be indicative for crystal defects in a sample, as fines can be caused by milling or grinding.

3.5. Binary mixtures

DSC results for binary mixtures are shown in Fig. 7. An effect of tablet filler on the thermal behavior of CBZ was observed. In presence of MCC, the intensity of the thermal events was reduced and broken peaks were visible around 190 °C. In presence of mannitol, a change in the thermal behavior of CBZ was observed. Mannitol melted around 164 °C and CBZ seemed to dissolve fully in melted mannitol of 30% drug load and partially at the higher drug loads resulting in a broadening of melting point for CBZ form III and a shift towards lower temperature around 172 °C compared to melting of pure form III at 176 °C. The same mixtures did not show any change in crystallinity in XRPD results (data not shown). Therefore, the interaction with mannitol is limited to temperatures of 164 °C and above. Also Joshi et al. (2002) reported the interaction of CBZ with mannitol as a temperature related phenomenon detected in DSC.

3.5.1. Drug release of binary mixtures

Drug release profiles of the binary mixtures comparing CBZ samples at same drug load are presented in Figs. 8 and 9 shows the comparison of drug release of different drug loads with CBZ B as an example. An overview of amount of CBZ released from the binary mixtures after 120 min dissolution test is shown in Table 4.

It is interesting to note that the variability in DIDR profiles found in the CBZ samples was present also in the drug release profiles of the binary mixtures. Amount of CBZ released after 120 min differed significantly among CBZ samples of the same drug load (ANOVA; $p < 0.001$, except for the 50% CBZ–MCC mixture). Difference in amount of drug dissolved among the various CBZ samples was much less with the presence of MCC than of mannitol. Methods for the analysis of dissolution curves were found to be either over discriminative, i.e., analysis by one-way repeated measures ANOVA

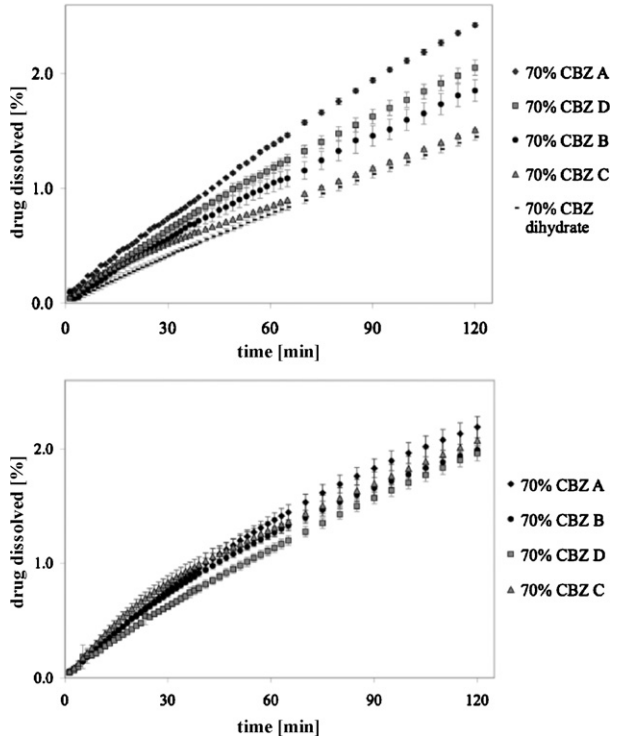

Fig. 8. Initial drug release profiles of binary mixtures at 70% drug load with mannitol (top) and with MCC (bottom).

(MANOVA), or not discriminative enough, i.e., difference factor (f_1) and similarity factor (f_2) proposed by FDA (1997).

Drug release profiles of binary mixtures showed dependance on drug load. Dissolution rate was increased at the lower drug loads of

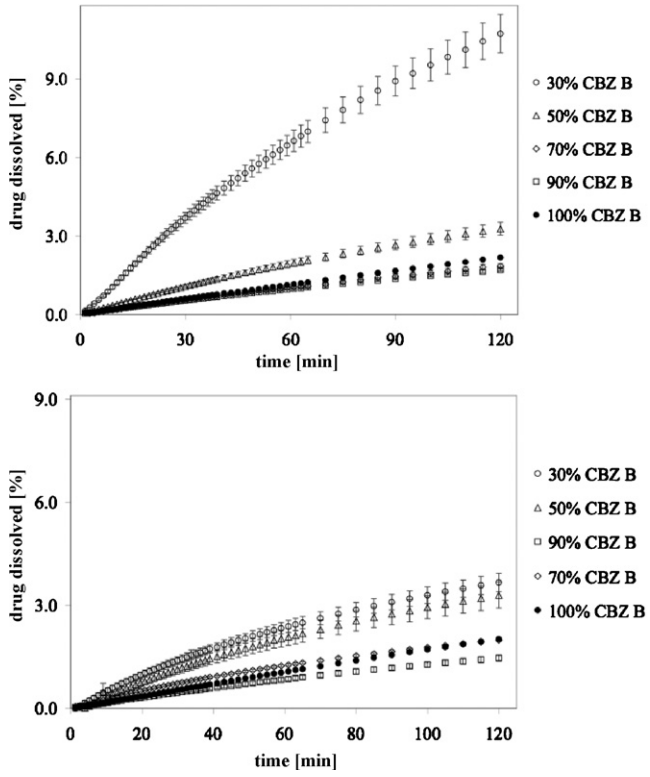

Fig. 9. Initial drug release profiles of binary mixture with mannitol (top) and with MCC (bottom).

Table 4
Amount of CBZ dissolved [%] from binary mixtures with mannitol and MCC at different drug loads after 120 min.

	Mannitol	MCC
30% CBZ		
A	16.06 ± 2.95	4.39 ± 0.22
B	10.73 ± 0.73	3.67 ± 0.27
C	13.39 ± 1.71	4.98 ± 0.08
D	10.61 ± 1.51	4.41 ± 0.28
50% CBZ		
A	3.70 ± 0.18	2.49 ± 0.56
B	3.28 ± 0.24	3.30 ± 0.37
C	2.58 ± 0.18	2.92 ± 0.59
D	3.33 ± 0.10	3.31 ± 0.39
70% CBZ		
A	1.85 ± 0.09	2.19 ± 0.09
B	2.05 ± 0.07	1.99 ± 0.04
C	2.43 ± 0.02	2.08 ± 0.12
D	1.52 ± 0.01	1.96 ± 0.07
90% CBZ		
A	2.00 ± 0.09	3.23 ± 0.26
B	1.70 ± 0.05	1.47 ± 0.09
C	1.47 ± 0.03	1.22 ± 0.01
D	1.63 ± 0.06	1.58 ± 0.10
100% CBZ		
A	2.33 ± 0.03	
B	2.18 ± 0.02	
C	1.39 ± 0.02	
D	2.17 ± 0.03	

50% and 30%, especially in binary mixtures with mannitol. Amount of drug dissolved was 2 times higher for compacts of 50% and 7–10 times higher for compacts of 30% drug load with mannitol. For all binary mixtures with 90% drug load, drug release was slower than for pure CBZ compacts.

A possible reason for the different effects of mannitol and MCC on drug release could be their solubility difference. Mannitol dissolved very fast compared to the drug. CBZ samples could express their dissolution variability, even at the lower drug loads, where mannitol enhanced the solubility of CBZ. In contrast, compacts with the insoluble MCC showed swollen surfaces with wide cracks after the drug release measurements. The fiber-like structure of MCC could form a matrix that was able to control the amount of CBZ released.

4. Conclusions

The unidirectional dissolution method proved to be a straightforward monitoring tool for preformulation studies. Commercial CBZ samples could be specified by two inflection points in the DIDR profiles reflecting the individual transformation to CBZ dihydrate. In presence of the excipient mannitol or MCC, variability among CBZ samples regarding drug release persited. However, high amount of mannitol strongly increased release rate of CBZ, and MCC was able to reduce the variability of CBZ samples. To control drug release and bioavailability of CBZ in tablet formulation, MCC is suggested as a suitable tablet filler.

Acknowledgments

The financial support by the Senglet Stiftung Basel, Switzerland, in form of a Ph.D. scholarship for Felicia Flicker is kindly appreciated. Acknowledgment has to be given to Dr. K. Chansanroj for her careful revision of this manuscript.

References

Al-Zein, H., Riad, L.E., Abd-Elbary, A., 1999. Effect of packaging and storage on the stability of carbamazepine tablets. Drug Dev. Ind. Pharm. 25, 223–227.

Blagden, N., de Matas, M., Gavan, P.T., York, P., 2007. Crystal engineering of active pharmaceutical ingredients to improve solubility and dissolution rates. Adv. Drug Deliv. Rev. 59, 617–630.
Bolourtchian, N., Nokhodchi, A., Dinarvand, R., 2001. The effect of solvent and crystallization conditions on habit modification of carbamazepine. Daru 9, 12–22.
Brittain, H.G., 2004. Fluorescence studies of the transformation of carbamazepine anhydrate form III to its dihydrate phase. J. Pharm. Sci. 93, 375–383.
Davidson, A., 1995. A multinational survey of the quatity of carbamazepine tablets. Drug Dev. Ind. Pharm. 21, 2167–2186.
FDA, 1997. Guidance for Industry: Dissolution Testing of Immediate Release Solid Oral Dosage Forms. Center for Drug Evaluation and Research, Rockville, MD, August.
Fleischman, S.G., Kuduva, S.S., McMahon, J.A., Moulton, B., Walsh, R.D.B., Rodrìguez-Hornedo, N., Zaworotko, M.J., 2003. Crystal engineering of the composition of pharmaceutical phases: multiple-component crystalline solids invloving carbamazepine. Cryst. Growth Des. 3, 909–919.
Getsoian, A., Lodaya, R., Blackburn, A., 2008. One-solvent polymorph screen of carbamazepine. Int. J. Pharm. 348, 3–9.
Gift, A.D., Luner, P.E., Luedeman, L., Taylor, L.S., 2008. Influence of polymeric excipients on crystal hydrate formation kinetics in aqueous slurries. J. Pharm. Sci. 97, 5198–5211.
Grzesiak, A.L., Lang, M., Kim, K., Matzger, A.J., 2003. Comparison of the four anhydrous polymorphs of carbamazepine and the crystal structure of form I. J. Pharm. Sci. 92, 2260–2271.
Hanson, R., Gray, V., 2004. Dissolution testing of solid dosage forms. In: Handbook of Dissolution Testing, 3rd ed. Dissolution Technologies, Inc., Hockessin, Delaware, pp. 33–71.
Joshi, B.V., Patil, V.B., Pokharkar, V.B., 2002. Compatibility studies between carbamazepine and tablet excipients using thermal and non-thermal methods. Drug Dev. Ind. Pharm. 28, 687–694.
Kipouros, K., Kachrimanis, K., Nikolakakis, I., Malamataris, S., 2005. Quantitative analysis of less soluble form IV in commercial carbamazepine (form III) by diffuse reflectance Fourier transform spectroscopy (DRIFTS) and lazy learning algorithm. Anal. Chim. Acta 550, 191–198.
Kobayashi, Y., Ito, S., Itai, S., Yamamoto, K., 2000. Physicochemical properties and bioavailability of carbamazepine polymorphs and dihydrate. Int. J. Pharm. 193, 137–146.
Krahn, F.U., Mielck, J.B., 1987. Relation between several polymorphic forms and the dihydrate of carbamazepine. Pharm. Acta Helv. 62, 247–254.
Krahn, F.U., Mielck, J.B., 1989. Effect of type and extent of crystalline order on chemical and physical stability of carbamazepine. Int. J. Pharm. 53, 25–34.
Laine, E., Tuominen, V., Ilvessalo, P., Kahela, P., 1984. Formation of dihydrate from carbamazepine anhydrate in aqueous conditions. Int. J. Pharm. 20, 307–314.
Lake, O.A., Olling, M., Barends, D.M., 1999. In vitro/in vivo correlations of dissolution data of carbamazepine immediate release tablets with pharmacokinetic data obtained in healthy volunteers. Eur. J. Pharm. Biopharm. 48, 13–19.
Lefebvre, C., Guyot-Hermann, A.M., Draguet-Brughmans, M., Bouch, R., Guyot, J.C., 1986. Polymorphic transitions of carbamazepine during grinding and compression. Drug Dev. Ind. Pharm. 12, 1913–1927.
Lehto, P., Aaltonen, J., Tenho, M., Rantanen, J., Hirvonen, J., Tanninen, V.P., Peltonen, L., 2008. Solvent-mediated solid phase transformations of carbamazepine: effects of simulated intestinal fluid and fasted state simulated intestinal fluid. J. Pharm. Sci. 98, 985–996.
Li, Y., Chow, P.S., Tan, R.B.H., Black, S.N., 2008. Effect of water activity on the transformation between hydrate and anhydrate of carbamazepine. Org. Process Res. Dev. 12, 264–270.
Lindenberg, M., Kopp, S., Dressman, J.B., 2004. Classification of orally administered drugs on the world health organization model list of essential medicines according to the biopharmaceutics classification system. Eur. J. Pharm. Biopharm. 58, 265–278.
Mahalaxmi, R., Ravikumar, Pandey, S., Shirwaikar, A., Shirwaikar, A., 2009. Effect of recrystallization on size, shape, polymorph and dissolution of carbamazepine. Int. J. PharmTech Res. 1, 725–732.
McGregor, C., Saunders, M.H., Buckton, G., Saklatvala, R.D., 2004. The use of high-speed differential scanning calorimetry (hyper-DSC) to study the thermal properties of carbamazepine polymorphs. Thermochim. Acta 417, 231–237.
McMahon, L.E., Timmins, P., Williams, A.C., York, P., 1996. Characterization of dihydrates prepared from carbamazepine polymorphs. J. Pharm. Sci. 85, 1064–1069.
Meyer, M.C., Staughn, A.B., Mhatre, R.M., Shah, V.P., Williams, R.L., Lesko, L.J., 1998. The relative bioavailability and in vivo–in vitro correlations for four marketed carbamazepine tablets. Pharm. Res. 15, 1787–1791.
Meyer, M.C., Straughn, A.B., Jarvi, E.J., Wood, G.C., Pelsor, F.R., Shah, V.P., 1992. The bioinequivalence of carbamazepine tablets with a history of clinical failures. Pharm. Res. 9, 1612–1616.
Mittapalli, P.K., Suresh, B., Hussaini, S.S.Q., Rao, Y.M., Apte, S., 2008. Comparative in vitro study of six carbamazepine products. AAPS PharmSciTech 9, 357.
Mosharraf, M., Sebhatu, T., Nyström, C., 1999. The effects of disordered structure on the solubility and dissolution rates of some hydrophilic, sparingly soluble drugs. Int. J. Pharm. 177, 29–51.
Murphy, D., Rodrguez-Cintrón, F., Langevin, B., Kelly, R.C., Rodrguez-Hornedo, N., 2002. Solution-mediated phase transformation of anhydrous to dihydrate carbamazepine and the effect of lattice disorder. Int. J. Pharm. 246, 121–134.
Otsuka, M., Ohfusa, T., Matsuda, Y., 2000. Effect of binders on polymorphic transformation kinetics of carbamazepine in aqueous solution. Colloids Surface 17, 145–152.
Qiu, Y., Chen, Y., Liu, L., Zhang, G.G.Z. (Eds.), 2009. Developing Solid Oral Dosage Forms: Pharmaceutical Theory and Practice, Solvates/Hydrates. Academic Press, pp. 32–34 (Chapter 2.3.2).
Qu, H., Louhi-Kultanen, M., Kallas, J., 2006. Solubility and stability of anhydrate/hydrate in solvent mixtures. Int. J. Pharm. 321, 101–107.
Rodrìguez-Hornedo, N., Murphy, D., 2004. Surfactant-facilitated crystallization of dihydrate carbamazepine during dissolution of anhydrous polymorph. J. Pharm. Sci. 93, 449–460.
Salameh, A.K., Taylor, L.S., 2006. Physical stability of crystal hydrates and their anhydrates in the presence of excipients. J. Pharm. Sci. 95, 446–461.
Suryanarayanan, R., 1989. Determination of the relative amounts of anhydrous carbamazepine ($C_{15}H_{12}N_2O$) and carbamazepine dihydrate ($C_{15}H_{12}N_2O{\cdot}2H_2O$) in a mixture by powder X-ray diffractometry. Pharm. Res. 6, 1017–1024.
Tian, F., Sandler, N., Gordon, K.C., McGoverin, C.M., Reay, A., Strachan, C.J., Saville, D.J., Rades, T., 2006a. Visualizing the conversion of carbamazepine in aqueous suspension with and without the presence of excipients: a single crystal study using sem and raman microscopy. Eur. J. Pharm. Biopharm. 64, 326–335.
Tian, F., Zeitler, J., Strachan, C., Saville, D., Gordon, K., Rades, T., 2006b. Characterizing the conversion kinetics of carbamazepine polymorphs to the dihydrate in aqueous suspension using raman spectroscopy. J. Pharm. Biomed. Anal. 40, 271–280.
Šehić, S., Betz, G., Š Hadžidedić, El-Arini, S.K., Leuenberger, H., 2010. Investigation of intrinsic dissolution behavior of different carbamazepine samples. Int. J. Pharm. 386, 77–90.
Wrolstad, R.E., Decker, E.A., Schwartz, S.J., Sporns, P., 2005. Measurement of water activity using isopiestic method. In: Handbook of Food Analytical Chemistry, Water, Proteins, Enzymes, Lipids, and Carbohydrates. Wiley-IEEE, p. 51 (Chapter A2.3).
Yu, L.X., Carlin, A.S., Amidon, G.L., Hussain, A.S., 2004. Feasibility studies of utilizing disk intrinsic dissolution rate to classify drugs. Int. J. Pharm. 270, 221–227.
Zakeri-Milani, P., Barzegar-Jalali, M., Azimi, M., Valizadeha, H., 2009. Biopharmaceutical classification of drugs using intrinsic dissolution rate (idr) and rat intestinal permeability. Eur. J. Pharm. Biopharm. 73, 102–106.
Zeitler, J.A., Taday, P.F., Gordon, K.C., Pepper, M., Rades, T., 2007. Solid-state transition mechanism in carbamazepine polymorphs by time-resolved terahertz spectroscopy. ChemPhysChem 8, 1924–1927.